Test particle limit for the pair structure of quenched-annealed fluid mixtures

Matthias Schmidt
Theoretische Physik II, Universität Bayreuth, D-95440 Bayreuth, Germany
and H. H. Wills Physics Laboratory, University of Bristol, Tyndall Avenue, Bristol BS8 1TL, United Kingdom
(Received 20 October 2008; revised manuscript received 23 February 2009; published 25 March 2009)

A density functional route to the pair structure of quenched-annealed fluid mixtures is presented. The bulk two-body partial pair correlation functions of the mixture are identified with the one-body density distributions in an external potential that models a fixed test particle. Quenched-annealed (replica) density functional theory is used to calculate the inhomogeneous one-body density distributions. A closed theory is obtained by using an exact sum rule that equates two different expressions for the cross pair correlation function between unlike species. Results for binary quenched-annealed hard sphere mixtures are found to agree well with computer simulation data, improving over results from the replica Ornstein-Zernike equations using the direct correlation functions, obtained as second functional derivatives of the quenched-annealed excess free energy functional, as input. The proposed framework allows for the independent determination of the blocked part of the fluid-fluid partial pair correlation function.

DOI: 10.1103/PhysRevE.79.031405 PACS number(s): 82.70.−y, 64.10.+h, 61.20.−p, 61.43.−j

I. INTRODUCTION

The behavior of liquids in confinement can differ dramatically from that in bulk [1,2]. One successful approach to study liquids confined in random porous media is based on quenched-annealed (QA) model fluid mixtures; see, e.g., [3–6]. The quenched components of such a mixture model a disordered solid, sharing the randomness of the pore structure as one important property with real porous substances. The annealed components of the QA mixture describe a fluid absorbed inside the random solid, and understanding its behavior constitutes the objective of the research. Work on QA models has been devoted to their structural correlations, phase behavior, and adsorption and desorption phenomena. Much of liquid state theory for equilibrium mixtures can be carried over to QA models. A primary theoretical tool is constituted by the replica trick, which enables one to obtain the properties of the QA system under consideration in the limit of vanishing number of replicated components of a suitably extended equilibrium (i.e., fully annealed) mixture. In particular, many of the equilibrium liquid state integral equation theories have been formulated for QA systems. The closure relation complements the replica Ornstein-Zernike relations [7–9] to form a closed theory. Such theories work inherently on the level of two-body correlation functions.

Density functional theory (DFT) is a powerful approach for the study of inhomogeneous equilibrium mixtures. In DFT the grand potential is expressed as a functional of the one-body density distributions [10,11]. In typical applications, one studies adsorption and phase behavior of liquids confined in pores with idealized (nonrandom) geometries, such as in planar slits. However, extending earlier approaches [12,13], it was shown that DFT can be formulated for QA mixtures [14]; a brief summary of this QA DFT (or replica DFT) is given below. The variational principle [14] for the disorder-averaged grand potential was derived using the replica procedure [15]. Lafuente and Cuesta gave an alternative derivation based on first principles [16], which has established the foundations of the QA DFT in a rigorous fashion.

As is common in DFT, application of the framework requires an approximation for the (in this case disorder-averaged) free energy functional. There is evidence, however, that obtaining QA functionals of acceptable quality is not more difficult than in the equilibrium case. Common approaches such as mean-field theory [17,18] and fundamental measure theory [14] have been used successfully. Several interesting problems were addressed in very simple model systems (see Ref. [19] for an overview). Comparison with computer simulation data has shown that the QA DFT yields semiquantitative to quantitative predictions for (disorder-averaged) inhomogeneous density profiles, partition coefficients, and phase boundaries. More recently the QA DFT has been applied to a range of interesting phenomena in complex models, such as capillary condensation in pores with rough walls [20], adsorption in slitlike pores modified with chain molecules as models for pillaredlike materials [21], adsorption on amorphous and microporous silica materials [18], adsorption in pillared slitlike pores [22], and adsorption on surfaces modified with brushlike chain structures [23]. Note, however, that while QA DFT yields properties averaged over the quenched disorder, it was convincingly argued that important phenomena such as hysteresis in sorption loops occur out of equilibrium [24–28].

Using the QA DFT, the bulk structure on the two-body level was investigated via the replica Ornstein-Zernike route. Two-body direct correlation functions can be obtained as second functional derivatives of the QA excess free energy functional. Inversion of the replica Ornstein-Zernike equations then yields the partial pair correlation functions. This route to the pair structure constitutes a demanding test for the quality of the approximation for the excess free energy functional, and comparison to simulation data showed satisfactory agreement, indicating the validity of the theory in principal [14]. It is to be noted that alternatives to the QA DFT have been proposed [29,30].

In this paper we show how to use the QA DFT to obtain bulk pair correlation functions from a test particle procedure. For equilibrium fluids this method is well established [31,32]: The one-body distribution of a fluid in the presence

 ©2009 The American Physical Society

of a (test) particle, which is fixed at the origin, is related to the (partial) two-body pair correlation functions in bulk; see, e.g., [33–35] for recent applications. Calculation of inhomogeneous density distributions constitutes a standard application of equilibrium DFT. Here we propose and test a similar procedure for QA mixtures. The generalization from equilibrium to QA mixtures is less straightforward than one might believe at first glance. The symmetry between cross correlation functions under exchange of species needs to be exploited (rather than to be used as a consistency check as is possible in the equilibrium case) in order to obtain a closed framework. Furthermore, we show that the blocked part of the fluid-fluid pair correlation function can be obtained independently.

The paper is organized as follows. In Sec. II the test particle theory is laid out, including a review of the binary case in equilibrium (Sec. II A), and the proposal for binary QA mixtures (Sec. II B), including the blocked part of the fluid-fluid pair correlation function (Sec. II C). The QA Widom-Rowlinson model is used to illustrate the theory (Sec. II D) and the generalization to multicomponent mixtures is presented (Sec. II E). In Sec. III results for the partial pair correlation functions of binary QA mixtures of hard spheres are presented and compared against simulation data. In Sec. IV conclusions are drawn.

II. DENSITY FUNCTIONAL THEORY

A. The binary case in equilibrium

We first review the test particle method in equilibrium. Consider a binary mixture of species 0 and 1 interacting with pair potentials $\phi_{ij}(r)$, where $i,j=0,1$ label the species and r is the center-center distance of the two particles considered. The system is characterized by microscopic density profiles $\rho_i(\mathbf{r})$ for species $i=0,1$, where $\mathbf{r}$ is the spatial coordinate. The grand potential as a functional of the one-body density distributions of the mixture is decomposed as

$$\tilde{\Omega}[\rho_0,\rho_1] = F^{\mathrm{exc}}[\rho_0,\rho_1] + \sum_{i=0,1} F^{\mathrm{id}}[\rho_i] + \sum_{i=0,1} \int d\mathbf{r}\rho_i(\mathbf{r})[V_i^{\mathrm{ext}}(\mathbf{r}) - \mu_i], \tag{1}$$

where the (exact) free energy functional of the ideal gas is $F^{\mathrm{id}}[\rho_i]=k_BT\int d\mathbf{r}\rho_i(\mathbf{r})\{\ln[\rho_i(\mathbf{r})\Lambda_i^3]-1\}$, with Λ_i being the (irrelevant) thermal de Broglie wave length of species $i=0,1$; k_B is the Boltzmann constant and T is absolute temperature; $V_i^{\mathrm{ext}}(\mathbf{r})$ is an external potential acting on species $i=0,1$, and μ_i is the corresponding chemical potential; $F^{\mathrm{exc}}[\rho_0,\rho_1]$ is the excess (over ideal gas) contribution to the (Helmholtz) free energy. The parametric dependence of $\tilde{\Omega}$ on T, μ_i, and system volume V is suppressed in the notation, as is the dependence of F^{exc} and F^{id} on T and V.

The variational principle [10] states that $\tilde{\Omega}$ is minimal at the true (equilibrium) density profiles, and hence

$$\frac{\delta\tilde{\Omega}[\rho_0,\rho_1]}{\delta\rho_i(\mathbf{r})} = 0, \quad i=0,1. \tag{2}$$

Introducing the one-body direct correlation functionals for each species $i=0,1$ via a functional derivative of the excess free energy functional,

$$c_i(\mathbf{r},[\rho_0,\rho_1]) = -\frac{\delta\beta F^{\mathrm{exc}}[\rho_0,\rho_1]}{\delta\rho_i(\mathbf{r})}, \tag{3}$$

where $\beta=1/(k_BT)$, allows us to write (2) as an implicit Euler-Lagrange equation for the one-body density profile,

$$\rho_i(\mathbf{r}) = \Lambda_i^{-3}\exp\{c_i(\mathbf{r},[\rho_0,\rho_1]) - \beta V_i^{\mathrm{ext}}(\mathbf{r}) + \beta\mu_i\}. \tag{4}$$

Pursuing the test particle route requires identification of the external potentials with the pair potentials, which models fixing a "test particle" of species $j=0,1$ (arbitrarily) at the origin. For fluid states spherical symmetry is imposed on the density distributions, such that the spatial dependence is only on $r=|\mathbf{r}|$. Setting $V_i^{\mathrm{ext}}(\mathbf{r})=\phi_{ij}(r)$ in (4), one obtains

$$\rho_i^{(j)}(r) = \Lambda_i^{-3}\exp\{c_i(r,[\rho_0^{(j)},\rho_1^{(j)}]) - \beta\phi_{ij}(r) + \beta\mu_i\}, \tag{5}$$

where $\rho_i^{(j)}(r)$ denotes the density profile of species i in the presence of a test particle of species j. The partial pair correlation functions are obtained by a normalization procedure,

$$g_{ij}(r) = \rho_i^{(j)}(r)/\rho_i^{(j)}(r\to\infty), \tag{6}$$

where $\rho_i^{(j)}(r\to\infty)\equiv\rho_i^{\mathrm{bulk}}$ is the bulk density of species i.

In particular, both $\rho_1^{(0)}(r)$ and $\rho_0^{(1)}(r)$ can be obtained from (5). Normalization via (6) then yields two different ways to obtain the cross pair correlation function. For the present case of a binary mixture, the nontrivial case of the general sum rule $g_{ij}(r)=g_{ji}(r)$ is

$$g_{01}(r) = g_{10}(r). \tag{7}$$

In general, when an approximate form of F^{exc} is used, (7) will be violated. The degree of violation constitutes a valuable measure for the quality of the approximation of F^{exc}. In practical applications, using accurate approaches such as fundamental measures theory, the error can be numerically remarkably small. See, e.g., the discussion in [36] of this issue for the (closely related) case of depletion potentials.

B. Quenched-annealed binary mixtures

The case of quenched-annealed mixtures possesses very different structure. Such systems are governed by *two* grand potential functionals $\tilde{\Omega}_0[\rho_0]$ and $\tilde{\Omega}_1[\rho_0,\rho_1]$, where the former determines the behavior of the quenched component 0, and the latter that of the annealed component 1 that is adsorbed in the matrix of the quenched species. The standard decomposition into ideal, excess, and external contributions reads

$$\tilde{\Omega}_0[\rho_0] = F^{\mathrm{id}}[\rho_0] + F_0^{\mathrm{exc}}[\rho_0] + \int d\mathbf{r}\,\rho_0(\mathbf{r})[V_0^{\mathrm{ext}}(\mathbf{r}) - \mu_0], \tag{8}$$

$$\tilde{\Omega}_1[\rho_0,\rho_1] = F^{\rm id}[\rho_1] + F_1^{\rm exc}[\rho_0,\rho_1] + \int d\mathbf{r}\, \rho_1(\mathbf{r})[V_1^{\rm ext}(\mathbf{r}) - \mu_1], \tag{9}$$

where $F_0^{\rm exc}[\rho_0]$ is the (equilibrium) excess free energy functional of the quenched component 0, and $F_1^{\rm exc}[\rho_0,\rho_1]$ is the disorder-averaged excess free energy functional of the annealed species 1, in the presence of species 0. The variational principle [14–16] implies the conditions

$$\frac{\delta\tilde{\Omega}_0[\rho_0]}{\delta\rho_0(\mathbf{r})} = 0, \tag{10}$$

$$\left.\frac{\delta\tilde{\Omega}_1[\rho_0,\rho_1]}{\delta\rho_1(\mathbf{r})}\right|_{\rho_0} = 0, \tag{11}$$

where $\rho_0(\mathbf{r})$ is solely determined by (10), and forms a fixed input quantity in (11). [Note that (8) and (10) constitute equilibrium DFT for a pure system and are recovered as the one-component limit of (1) and (2), respectively.]

The one-body direct correlation functionals for the QA system are obtained as first functional derivatives,

$$c_0(\mathbf{r},[\rho_0]) = -\frac{\delta\beta F_0^{\rm exc}[\rho_0]}{\delta\rho_0(\mathbf{r})}, \tag{12}$$

$$c_1(\mathbf{r},[\rho_0,\rho_1]) = -\frac{\delta\beta F_1^{\rm exc}[\rho_0,\rho_1]}{\delta\rho_1(\mathbf{r})}. \tag{13}$$

More explicitly, the Euler-Lagrange equations are obtained from inserting the decomposition (8) and (9) of the grand potential functionals into the minimization conditions (10) and (11); use of the definitions (12) and (13) then yields

$$\rho_0(\mathbf{r}) = \Lambda_0^{-3}\exp\{c_0(\mathbf{r},[\rho_0]) - \beta V_0^{\rm ext}(\mathbf{r}) + \beta\mu_0\}, \tag{14}$$

$$\rho_1(\mathbf{r}) = \Lambda_1^{-3}\exp\{c_1(\mathbf{r},[\rho_0,\rho_1]) - \beta V_1^{\rm ext}(\mathbf{r}) + \beta\mu_1\}. \tag{15}$$

The framework outlined so far is general and applies to arbitrary forms of the external potentials $V_i^{\rm ext}(\mathbf{r})$ acting on species $i=0,1$.

For a test particle calculation, the external potential needs to be identified with the pair interaction potentials $\phi_{ij}(r)$. As in the equilibrium case, one aims at modeling a fixed test particle of species j at the origin. We first consider the matrix particles only, $j=0$, and require that $V_0(\mathbf{r})=\phi_{00}(r)$. Hence, from (14) one obtains

$$\rho_0^{(0)}(r) = \Lambda_0^{-3}\exp\{c_0(r,[\rho_0^{(0)}]) - \beta\phi_{00}(r) + \beta\mu_0\}, \tag{16}$$

which is equivalent to the self-consistency equation for $\rho_0^{(0)}(r)$ in the equilibrium (fully annealed) case, e.g., as obtained from (5) for the case of a pure system.

In the second step, we determine the fluid density profile by choosing again a matrix particle as the test particle, $j=0$; this amounts to setting $V_1^{\rm ext}(\mathbf{r})=\phi_{01}(r)$ in (15). This yields

$$\rho_1^{(0)}(r) = \Lambda_1^{-3}\exp\{c_1(r,[\rho_0^{(0)},\rho_1^{(0)}]) - \beta\phi_{01}(r) + \beta\mu_1\}, \tag{17}$$

which determines $\rho_1^{(0)}(r)$ uniquely when using $\rho_0^{(0)}(r)$, as obtained from (16), as an input quantity.

In the third step, we fix a *fluid* particle at the origin, $j=1$, and calculate the density profile of the surrounding fluid of species 1. This requires setting $V_1^{\rm ext}(\mathbf{r})=\phi_{11}(r)$ in (15). The matrix density distribution is required as an input, here around the test particle of species 1, i.e., $\rho_0^{(1)}(r)$. In the current framework, this is not a directly accessible quantity. In order to make progress, note that both the definition of the partial pair correlation functions (6) and the symmetry relationship (7) still hold in the QA case. Combining these yields

$$\rho_0^{(1)}(r) = \frac{\rho_0^{\rm bulk}}{\rho_1^{\rm bulk}}\rho_1^{(0)}(r), \tag{18}$$

where the right-hand side consists of known quantities only. [Recall that $\rho_1^{(0)}$ is obtained from (17).] This allows us to rewrite (15) as

$$\rho_1^{(1)}(r) = \Lambda_1^{-3}\exp\{c_1(r,[\rho_0^{(1)},\rho_1^{(1)}]) - \beta\phi_{11}(r) + \beta\mu_1\}, \tag{19}$$

which forms a closed equation for $\rho_1^{(1)}(r)$. Trivial normalization of $\rho_0^{(0)}(r)$, $\rho_0^{(1)}(r)$, and $\rho_1^{(1)}(r)$ via (6) yields $g_{00}(r)$, $g_{01}(r)$, and $g_{11}(r)$, respectively.

C. The blocked part of the fluid-fluid pair correlation function

The pair correlation function between particles of different replicas is commonly referred to as the blocked (or blocking) part of the (fluid-fluid partial) pair correlation function, $g_b(r)$. The authors of Ref. [16] have argued that the corresponding blocked direct correlation function, $c_b(r)$, cannot be obtained as a second functional derivative in the QA DFT framework, and that the situation is consistent with the fact that the (bulk) thermodynamics of QA mixtures can be obtained solely from the connected two-body correlation functions [9]. As we demonstrate in the following, the test particle procedure offers a natural route to $g_b(r)$, via the identification with the (normalized) fluid density profile around a test particle of a replica different from that of the fluid.

Although the definition of $g_b(r)$ within the replica framework may seem somewhat formal at first glance, there is a direct probabilistic interpretation, which allows its determination, say in a computer simulation or in an experiment [37–39]. Up to a normalization constant, $g_b(r)$ is the joint probability of finding a pair of particles at distance r, with the members of the pair belonging to different fluid configurations. Nontrivial correlations arise from the fact that the two different fluid configurations are exposed to the same matrix configuration. Loosely speaking, the presence of a fluid particle (say at $\mathbf{r}_1$) is accompanied by the presence of a large enough "hole" in the matrix to accommodate this particle. The hole in turn affects the density (at $\mathbf{r}_2$, with $r=|\mathbf{r}_1-\mathbf{r}_2|$) of the fluid particles in a different replica. This indirect influence is present despite the absence of direct interactions between particles of different replicas.

The implementation in the test particle framework is straightforward. We are seeking to obtain the density profile of the annealed species 1. The test particle is taken to be of species 1, but as it belongs to a different fluid configuration (to a different replica in the replica picture) it does not interact with the fluid of species 1 and the corresponding external potential vanishes, $V_1^{\rm ext}(r)=0$. Nevertheless, having chosen the position of the test particle as the origin leads to an inhomogeneous density profile of matrix particles, $\rho_0^{(1)}(r)$. This is known from (17) and (18), and constitutes the sole inhomogeneity-inducing influence on the fluid of species 1. Hence the fluid density profile $\rho_{1b}^{(1)}(r)$ in this situation is obtained from specializing the general Euler-Lagrange equation (15) as

$$\rho_{1b}^{(1)}(r) = \Lambda_1^{-3}\exp\{c_1(r,[\rho_0^{(1)},\rho_{1b}^{(1)}]) + \beta\mu_1\}. \tag{20}$$

Application of the normalization procedure (6) yields

$$g_b(r) = \rho_{1b}^{(1)}(r)/\rho_{1b}^{(1)}(r\to\infty). \tag{21}$$

D. Quenched-annealed Widom-Rowlinson model as an illustration

A minimalistic model is the QA analog of the (equilibrium) Widom-Rowlinson (WR) model [40], namely, an ideal gas of quenched matrix particles in which an annealed ideal gas is adsorbed; the only nonvanishing (pair) interaction is that between particles of unlike species, taken as hard core repulsion with range σ_{01}. While the equilibrium Widom-Rowlinson model constitutes a nontrivial many-body problem and displays a demixing phase transition (see, e.g., [41] for a recent study), the QA version has only a single phase and the replica Ornstein-Zernike equations can be solved exactly [42].

Following Ref. [16] we start from the excess free energy functionals for the matrix $F_0^{\rm exc}[\rho_0]=0$ and for the fluid $F_1^{\rm exc}[\rho_0,\rho_1]=-k_BT\int d\mathbf{r}\,d\mathbf{r}'\rho_0(\mathbf{r})\rho_1(\mathbf{r}')f_{01}(|\mathbf{r}-\mathbf{r}'|)$, where the Mayer function $f_{01}(r)=\exp[-\beta\phi_{01}(r)]-1$ equals -1 for center-center separations $r<\sigma_{01}$ and vanishes otherwise. The form of $F_1^{\rm exc}[\rho_0,\rho_1]$ is identical to that obtained by the fundamental-measure theory for quenched-annealed systems [14] (but is different from the fundamental-measure DFT for the equilibrium WR model [43]). The behavior of the matrix alone is trivial: Its one-body direct correlation function, formally obtained via (12), is $c_0(r)=0$. Fixing a test matrix particle does not exert an influence on the other matrix particles; hence $\phi_{00}(r)=0$ and (16) leads to $\rho_0^{(0)}(r)=\Lambda_0^{-3}\exp(\beta\mu_0)$. Normalization via (6) gives $g_{00}(r)=1$, as expected.

The one-body direct correlation function of the fluid, obtained via functional differentiation (13), is given by $c_1(r',[\rho_0])=\int d\mathbf{r}\,\rho_0(\mathbf{r})f_{01}(|\mathbf{r}-\mathbf{r}'|)$, where $r'=|\mathbf{r}'|$; this is independent of the functional form of $\rho_1(\mathbf{r})$. In the case of the test particle being of the matrix species $c_1(r',[\rho_0^{(0)}])=\rho_0\int d\mathbf{r}\,f_{01}(|\mathbf{r}-\mathbf{r}'|)=-4\pi\sigma_{01}^3\rho_0/3$. From the test particle equation (17) one obtains $\rho_1^{(0)}(r)=\Lambda_1^{-3}\exp[\beta\mu_1-(4\pi/3)\sigma_{01}^3\rho_0][1+f_{01}(r)]$, where because of the hard core nature of the matrix-fluid interaction $\exp[-\beta\phi_{01}(r)]=1+f_{01}(r)$. Normalization via (6) and use of the species exchange symmetry (7) yields $g_{10}(r)=g_{01}(r)=1+f_{01}(r)$.

The one-body direct correlation function for the fluid (13) is given by $c_1(r')=c_1(r',[\rho_0(1+f_{01}(r))])=\rho_0\int d\mathbf{r}\,f_{01}(|\mathbf{r}-\mathbf{r}'|)[1+f_{01}(|\mathbf{r}|)]=(4\pi/3)\rho_0\sigma_{01}^3+\rho_0O(r')$, where $O(r')$ is the overlap (intersection volume) of two spheres of radius σ_{01}, given by $O(r')=\int d\mathbf{r}\,f_{01}(|\mathbf{r}|)f_{01}(|\mathbf{r}-\mathbf{r}'|)$, and more explicitly as $O(r')=(\pi/12)(r'-2\sigma_{01})^2(r'+4\sigma_{01})$ for $r'<2\sigma_{01}$ and zero otherwise. The fact that $\phi_{11}(r)=0$ renders Eqs. (19) and (20) identical, from which $g_{11}(r)=g_b(r)$ follows. Explicitly, $\rho_1^{(1)}(r)=\Lambda_1^{-3}\exp[\beta\mu_1-(4\pi/3)\rho_0\sigma_{01}^3]\exp[\rho_0O(r)]$, which upon normalization (6) yields $g_{11}(r)=\exp[\rho_0O(r)]$. This fully specifies the exact pair structural correlation functions [42]. For completeness, one can use the replica Ornstein-Zernike equations [42] to obtain the two-body direct correlation function between fluid and matrix, $c_{10}(r)=f_{10}(r)$, and the connected and blocked parts of the fluid-fluid direct correlation function, $c_c(r)=0$ and $c_b(r)=\exp[\rho_0O(r)]-1-\rho_0O(r)$, respectively.

E. Generalization to the multicomponent case

The test particle procedure applies in a straightforward way to QA mixtures with more than two components (albeit at the expense of notational burdens). We consider m_0+m_1 components, where species $i=1,\ldots,m_0$ are quenched and species $i=m_0+1,\ldots,m_0+m_1$ are annealed. The aim is to calculate the $(m_0+m_1)\times(m_0+m_1)$ matrix of partial pair correlation functions, written in block matrix form as

$$\begin{pmatrix}\mathbf{g}_{00}(r) & \mathbf{g}_{01}(r)\\ \mathbf{g}_{10}(r) & \mathbf{g}_{11}(r)\end{pmatrix}, \tag{22}$$

where $\mathbf{g}_{\alpha\gamma}(r)$ indicates the sub-blocks with $\alpha,\gamma=0,1$, referring to quenched (0) and annealed (1) species. $\mathbf{g}_{00}(r)$ is the $m_0\times m_0$ matrix with elements $g_{ij}(r)$, $1\leqslant i,j\leqslant m_0$, and similarly for the other blocks in (22).

Obtaining $\mathbf{g}_{00}(r)$ is straightforward in principle, as this constitutes the multicomponent version of the equilibrium problem described in Sec. II A. Normalization of the one-body density distributions $\rho_i^{(j)}(r)$ as obtained via the multicomponent version of (16) yields $g_{ij}(r)$ via (6) for $1\leqslant i,j\leqslant m_0$, i.e., for pairs of particles of quenched species.

In the second step, particles of the quenched species $j=1,\ldots,m_0$ are (again) successively used as test particles; this allows the density distributions $\rho_i^{(j)}(r)$ of the annealed components $i=m_0+1,\ldots,m_0+m_1$ to be obtained via the multicomponent version of (17). These density profiles, when normalized (6), constitute the block matrix $\mathbf{g}_{10}(r)$ in (22). Transposition of this result (indicated by the superscript T) immediately gives

$$\mathbf{g}_{01}(r) = \mathbf{g}_{10}^T(r), \tag{23}$$

which amounts to the componentwise identification of the inhomogeneous one-body densities

$$\rho_j^{(i)}(r) = \frac{\rho_j^{\rm bulk}}{\rho_i^{\rm bulk}}\rho_i^{(j)}(r), \tag{24}$$

where $1\leqslant j\leqslant m_0$ and $m_0+1\leqslant i\leqslant m_0+m_1$.

Next the test particle j is successively taken to be of the annealed species, i.e., $j=m_0+1,\ldots,m_0+m_1$, and $\rho_i^{(j)}(r)$ is ob-

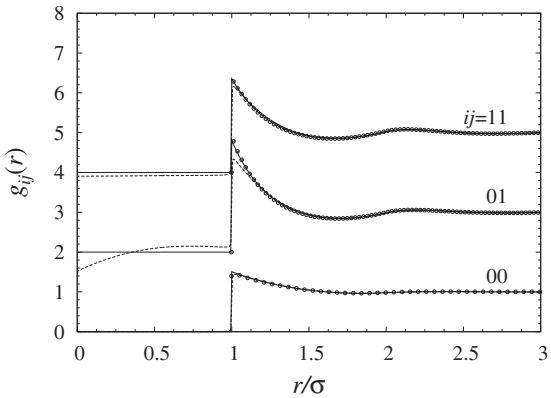

FIG. 1. Partial pair correlation functions $g_{00}(r)$, $g_{01}(r)$, and $g_{11}(r)$ as functions of the scaled distance r/σ for a QA binary hard sphere mixture of quenched species 0 and annealed species 1 with equal sizes, $\sigma_0=\sigma_1\equiv\sigma$, and equal packing fractions, $\eta_0=\eta_1=0.15$. Shown are results obtained by the test particle approach (solid lines), from Monte Carlo computer simulations (symbols) [14], and from the replica Ornstein-Zernike route (dashed lines) [14]. Results for $g_{01}(r)$ and $g_{11}(r)$ are shifted upward by two and four units, respectively, for clarity.

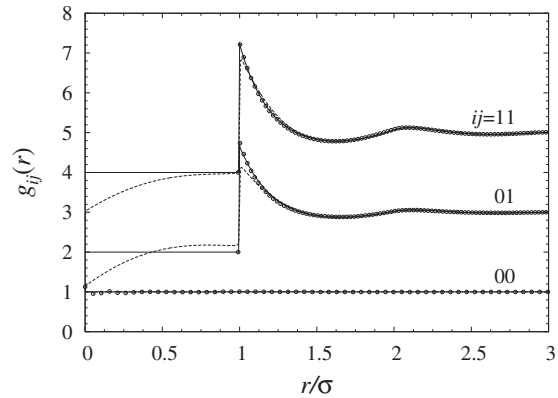

FIG. 2. Same as Fig. 1 but for annealed hard spheres (species 1) immersed in a quenched matrix of freely overlapping spheres (species 0) with equal sizes $\sigma_0=\sigma_1$ and equal packing fractions $\eta_0=\eta_1=0.2$.

tained for all annealed components $i=m_0+1,\ldots,m_0+m_1$, again via the multicomponent version of the Euler-Lagrange equation (19). Normalizing via (6) yields $\mathbf{g}_{11}(r)$, which fully specifies (22). For the case of blocked correlation functions the matrix $\mathbf{g}_{11}(r)$ in (22) is replaced with the matrix of blocked correlation functions, $\mathbf{g}_b(r)$, which can be obtained componentwise via the multicomponent version of (20) and (21).

III. RESULTS: QUENCHED-ANNEALED HARD SPHERE MIXTURES

As a test we apply the framework developed above to QA mixtures of hard spheres with packing fractions $\eta_i=\pi\rho_i^{\text{bulk}}\sigma_i^3/6$, where σ_i is the hard core diameter of species $i=0,1$. In the first case the interactions are additive such that a pair of particles 0 and 1 exhibits hard core exclusion at a distance $(\sigma_0+\sigma_1)/2$. For this system, the fundamental measure approach of [14] yields a QA excess free energy functional $F_1^{\text{exc}}[\rho_0,\rho_1]=F_{\text{hs}}^{\text{exc}}[\rho_0,\rho_1]-F_{\text{hs}}^{\text{exc}}[\rho_0]$, where $F_{\text{hs}}^{\text{exc}}$ is Rosenfeld's equilibrium excess free energy functional for additive hard sphere mixtures [44]. For the quenched species simply $F_0^{\text{exc}}[\rho_0]=F_{\text{hs}}^{\text{exc}}[\rho_0]$. The numerical solution of (16), (17), (19), and (20), is performed with standard Picard iteration.

Figure 1 displays results from the present theory along with the Monte Carlo simulation data of Ref. [14] for the case of equal sizes $\sigma_0=\sigma_1$ and packing fractions $\eta_0=\eta_1=0.15$. Excellent agreement of theoretical and simulation data is found. The core condition, $g_{ij}(r<\sigma_{ij})=0$, is satisfied by construction, as can be inferred from (16), (17), and (19), by noting that $\phi_{ij}(r<\sigma_{ij})=\infty$ and that c_0 and c_1 are finite.

In our second case, the matrix-matrix interaction is taken to be ideal, such that matrix particles can freely overlap with other matrix particles. This corresponds to a QA Asakura-Oosawa model (see, e.g., Ref. [45], and references therein) where the polymers (species 0) are quenched and the colloids (species 1) are annealed. The QA excess free energy functional F_1^{exc} for this case differs both from the hard sphere case and from the (approximative) equilibrium Asakura-Oosawa functional [46]. As a consequence, the matrix-matrix correlations are those of an ideal gas, $g_{00}=1$, and $\rho_0^{(0)}(r)=\rho_0^{\text{bulk}}$. Results for packing fractions $\eta_0=\eta_1=0.2$ and $\sigma_0=\sigma_1$ are shown in Fig. 2. Again very good agreement with the simulation data is found.

As can be gleaned from Figs. 1 and 2, the results from the test particle method are more accurate at small separations than those obtained from the replica Ornstein-Zernike equations and the two-body direct correlation functions from second functional derivatives of the quenched-annealed free energy functional; Ref. [14] gives details of this approach. The origin of the differences lies in the fact that second rather than first derivatives [Eqs. (12) and (13)] of the excess free energy functional enter into the framework. The Ornstein-Zernike route constitutes a valuable test bed to assess the quality of the approximation to the QA excess free energy functional. In practical applications, the test particle method presented here yields superior results—at the expense of more numerical work.

Finally, we display results for the blocked part of the fluid-fluid partial pair correlation function, $g_b(r)$, for both types of matrices considered in Fig. 3. We restrict ourselves to slightly smaller overall packing fractions in order to alleviate problems of insufficent equilibration of the simulation runs, to which we found $g_b(r)$ to be particularly susceptible. For the cases shown, very good quantitative agreement of simulation data and theoretical results can be observed. Note the marked qualitative difference of the shape of $g_{11}(r)$, shown in Fig. 2, as compared to $g_b(r)$. The former features a hard core exclusion region due to the presence of fluid-fluid interactions in (19), while the latter indicates strong clustering of particles, due to the absence of direct fluid-fluid interactions in (20). Both pair correlation functions display oscillatory behavior at larger distances, but with much smaller amplitude in the case of $g_b(r)$. For comparison, we also display the result for the QA Widom-Rowlinson model (Sec.

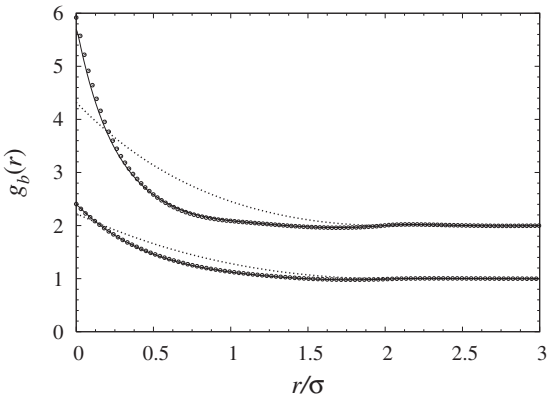

FIG. 3. Blocked part of the fluid-fluid partial pair correlation function, $g_b(r)$, as a function of the scaled distance r/σ, as obtained from the test particle method (solid lines) and from computer simulations (symbols). Results are shown for annealed hard spheres immersed in a quenched matrix of freely overlapping spheres with equal sizes $\sigma_0=\sigma_1\equiv\sigma$ and equal packing fractions $\eta_0=\eta_1=0.1$ and 0.15 (the latter shifted upwards by one unit). Also shown is the analytic result for the quenched-annealed WR model (dotted lines) for the same parameters.

II D) in Fig. 3, $g_b(r)=\exp[\rho_0 O(r)]$; the sizes are chosen to be the same as in the case of the hard sphere fluid, $\sigma_{01}=\sigma_1$. The correlation function reaches a smaller maximum value at $r=0$ and decays more slowly with distance for separation distances $r<2\sigma_{01}$. Beyond this limiting distance $g_b(r>2\sigma)=0$, whereas damped oscillatory decay is apparent in the case of the hard sphere fluid.

IV. CONCLUSIONS

In conclusion, we have shown that a test particle procedure can be used in order to calculate all partial pair correlation functions of QA binary and multicomponent mixtures. For test cases of binary mixtures with hard core interactions, we found that numerical results from this approach compare very well with Monte Carlo simulation data.

We have restricted ourselves to the simplest case of QA mixtures of spherical particles. In principle the framework can be generalized in a straightforward way to inhomogeneous liquids and to crystals, as well as to more complicated models with orientation-dependent interactions. In future work, it would be interesting to assess the quality of the approach against results from integral equation theory based on the replica Ornstein-Zernike equations, as well as to investigate the behavior of the QA hard sphere models at yet higher packing fractions than those considered in the present paper. In particular, addressing questions of the asymptotic decay of correlation functions [47,48] constitutes an interesting topic. Also of interest is the dynamical behavior of correlation functions [49] and questions addressing fluid diffusivity in random media [50].

ACKNOWLEDGMENT

I am grateful to Professor Thomas M. Fischer for several inspiring discussions on the topic of this paper. This work was supported by the EPSRC.

[1] R. Evans, J. Phys.: Condens. Matter **2**, 8989 (1990).
[2] L. D. Gelb, K. E. Gubbins, R. Radhakrishnan, and M. Sliwinska-Bartkowiak, Rep. Prog. Phys. **62**, 1573 (1999).
[3] O. Pizio, A. Patrykiejew, and S. Sokołowski, J. Phys. Chem. C **111**, 15743 (2007).
[4] O. Pizio, M. Borówko, W. Rzysko, T. Staszewski, and S. Sokołowski, J. Chem. Phys. **128**, 044702 (2008).
[5] E. Paschinger and G. Kahl, Phys. Rev. E **61**, 5330 (2000).
[6] E. Paschinger, D. Levesque, G. Kahl, and J. J. Weis, Europhys. Lett. **55**, 178 (2001).
[7] W. G. Madden and E. D. Glandt, J. Stat. Phys. **51**, 537 (1988).
[8] J. A. Given and G. Stell, J. Chem. Phys. **97**, 4573 (1992).
[9] M. L. Rosinberg, G. Tarjus, and G. Stell, J. Chem. Phys. **100**, 5172 (1994).
[10] R. Evans, Adv. Phys. **28**, 143 (1979).
[11] R. Evans, in *Fundamentals of Inhomogeneous Fluids*, edited by D. Henderson (Dekker, New York, 1992), Chap. 3, p. 85.
[12] G. I. Menon and C. Dasgupta, Phys. Rev. Lett. **73**, 1023 (1994).
[13] F. Thalmann, C. Dasgupta, and D. Feinberg, Europhys. Lett. **50**, 54 (2000).
[14] M. Schmidt, Phys. Rev. E **66**, 041108 (2002).
[15] H. Reich and M. Schmidt, J. Stat. Phys. **116**, 1683 (2004).
[16] L. Lafuente and J. A. Cuesta, Phys. Rev. E **74**, 041502 (2006).
[17] A. J. Archer, M. Schmidt, and R. Evans, Phys. Rev. E **73**, 011506 (2006).
[18] P. I. Ravikovitch and A. V. Neimark, Langmuir **22**, 11171 (2006).
[19] M. Schmidt, J. Phys.: Condens. Matter **17**, S3481 (2005).
[20] P. Bryk, W. Rzysko, A. Malijevsky, and S. Sokołowski, J. Colloid Interface Sci. **313**, 41 (2007).
[21] M. Matusewicz, A. Patrykiejew, S. Sokołowski, and O. Pizio, J. Chem. Phys. **127**, 174707 (2007).
[22] Z. Sokołowska and S. Sokołowska, J. Colloid Interface Sci. **316**, 652 (2007).
[23] A. Patrykiejew, S. Sokołowski, R. Tscheliessnig, and J. Fischer, J. Phys. Chem. B **112**, 4552 (2008).
[24] E. Kierlik, P. A. Monson, M. L. Rosinberg, L. Sarkisov, and G. Tarjus, Phys. Rev. Lett. **87**, 055701 (2001).
[25] E. Kierlik, P. A. Monson, M. L. Rosinberg, and G. Tarjus, J. Phys.: Condens. Matter **14**, 9295 (2002).
[26] M. L. Rosinberg, E. Kierlik, and G. Tarjus, Europhys. Lett. **62**, 377 (2003).
[27] F. Detcheverry, E. Kierlik, M. L. Rosinberg, and G. Tarjus, Phys. Rev. E **68**, 061504 (2003).
[28] L. Sarkisov and P. A. Monson, Phys. Rev. E **65**, 011202 (2001).
[29] E. A. Ustinov and D. D. Do, Adsorption **11**, 455 (2005).
[30] E. A. Ustinov, D. D. Do, and J. Jaroniec, Langmuir **22**, 6238 (2006).

[31] J. K. Percus, Phys. Rev. Lett. **8**, 462 (1962).
[32] J. P. Hansen and I. R. McDonald, *Theory of Simple Liquids*, 3rd ed. (Academic, London, 2006).
[33] C. Grodon, M. Dijkstra, R. Evans, and R. Roth, J. Chem. Phys. **121**, 7869 (2004).
[34] C. Grodon, M. Dijkstra, R. Evans, and R. Roth, Mol. Phys. **103**, 3009 (2005).
[35] J. Baumgartl, R. P. A. Dullens, M. Dijkstra, R. Roth, and C. Bechinger, Phys. Rev. Lett. **98**, 198303 (2007).
[36] R. Roth, R. Evans, and S. Dietrich, Phys. Rev. E **62**, 5360 (2000).
[37] One could envisage a real space analysis of a quenched-annealed colloidal dispersion [38,39], where the correlation functions are obtained from coordinate tracking of particle positions.
[38] G. Cruz de León, J. M. Saucedo-Solorio, and J. L. Arauz-Lara, Phys. Rev. Lett. **81**, 1122 (1998).
[39] G. Cruz de León and J. L. Arauz-Lara, Phys. Rev. E **59**, 4203 (1999).
[40] B. Widom and J. S. Rowlinson, J. Chem. Phys. **52**, 1670 (1970).
[41] J. M. Brader and R. L. C. Vink, J. Phys.: Condens. Matter **19**, 036101 (2007).
[42] E. Lomba, J. A. Given, G. Stell, J. J. Weis, and D. Levesque, Phys. Rev. E **48**, 233 (1993).
[43] M. Schmidt, Phys. Rev. E **63**, 010101(R) (2000).
[44] Y. Rosenfeld, Phys. Rev. Lett. **63**, 980 (1989).
[45] M. Dijkstra, J. M. Brader, and R. Evans, J. Phys.: Condens. Matter **11**, 10079 (1999).
[46] The main qualitative difference from the hard sphere case is a shift of the singularity at packing fraction unity to a lower value of $\exp(-\eta_0)$; for details see Ref. [14].
[47] R. Evans, J. R. Henderson, D. C. Hoyle, A. O. Parry, and Z. A. Sabeur, Mol. Phys. **80**, 755 (1993).
[48] R. Evans, R. J. F. Leote de Carvalho, J. R. Henderson, and D. C. Hoyle, J. Chem. Phys. **100**, 591 (1994).
[49] A. J. Archer, P. Hopkins, and M. Schmidt, Phys. Rev. E **75**, 040501(R) (2007).
[50] J. Mittal, J. R. Errington, and T. M. Truskett, Phys. Rev. E **74**, 040102(R) (2006).